Effect of Electron Correlations on Magnetic Excitations in the Isovalently Doped Iron-Based Superconductor $Ba(Fe_{1-x}Ru_x)_2As_2$

Jun Zhao,[1,2,3] C. R. Rotundu,[4] K. Marty,[5] M. Matsuda,[5] Y. Zhao,[6,7] C. Setty,[8] E. Bourret-Courchesne,[4] Jiangping Hu,[8] and R. J. Birgeneau[2,9]

[1]*Department of Physics, and Laboratory of Advanced Materials, State Key Laboratory of Surface Physics, Fudan University, Shanghai 200433, People's Republic of China*
[2]*Department of Physics, University of California, Berkeley, California 94720, USA*
[3]*Miller Institute for Basic Research in Science, Berkeley, California 94720, USA*
[4]*Materials Sciences Division, Lawrence Berkeley National Laboratory, Berkeley, California 94720, USA*
[5]*Oak Ridge National Laboratory, Oak Ridge, Tennessee 37831, USA*
[6]*NIST Center for Neutron Research, National Institute of Standards and Technology, Gaithersburg, Maryland 20899, USA*
[7]*Department of Materials Science and Engineering, University of Maryland, College Park, Maryland 20742, USA*
[8]*Department of Physics, Purdue University, West Lafayette, Indiana 47907, USA*
[9]*Department of Materials Science and Engineering, University of California, Berkeley, California 94720, USA*

(Received 12 January 2012; published 5 April 2013)

Magnetic correlations in isovalently doped $Ba(Fe_{1-x}Ru_x)_2As_2$ ($x = 0.25$, $T_c = 14.5$ K; $x = 0.35$, $T_c = 20$ K) are studied by elastic and inelastic neutron scattering techniques. A relatively large superconducting spin gap accompanied by a weak resonance mode is observed in the superconducting state in both samples. In the normal state, the magnetic excitation intensity is dramatically reduced with increasing Ru doping toward the optimally doped regime. Our results favor that the weakening of the electron-electron correlations by Ru doping is responsible for the dampening of the resonance mode, as well as the suppression of the normal state antiferromagnetic correlations near the optimally doped regime in this system.

DOI: 10.1103/PhysRevLett.110.147003 PACS numbers: 74.25.Ha, 74.70.−b, 78.70.Nx

The parent compounds of the cuprate high T_c superconductors are Mott insulators. Superconductivity only appears after sufficient carriers are introduced though heterovalent doping [1]. Conversely, the parent compounds of the iron-based superconductors are antiferromagnetic semimetals, which naturally suggest that the electron correlations in the iron-based materials are weaker than those of the cuprates. The moderately correlated iron-based superconductors exhibit remarkably rich phase diagrams: superconductivity can be obtained through carrier doping (heterovalent), application of pressure, or isovalent doping [2]. $Ba(Fe_{1-x}Ru_x)_2As_2$ is a prototypical isovalently doped superconductor, as Ru has a similar electronic configuration to that of Fe and therefore, is not expected to introduce extra electrons or holes. Ru doping suppresses the static magnetic order much more gradually than is observed in the electron doped compounds. The magnetic and structural (orthorhombic to tetragonal) phase transitions coincide in temperature over the whole phase diagram [Fig. 1(a)], much different from the electron doped compounds where the structural and magnetic phase transitions separate for certain dopant concentrations [3,4]. Therefore, understanding the interplay between the electronic structure, magnetism, and superconductivity in isovalently doped iron-based superconductors is particularly interesting because they may provide a new route to the understanding of high T_c superconductivity.

The evolutions of the band structures and antiferromagnetism in carrier doped iron-based materials have been well documented. It has been suggested that the superconductivity is enhanced by the Fermi surface nesting, because the T_c decreases when the mismatch of the electron and hole Fermi surface increases with carrier

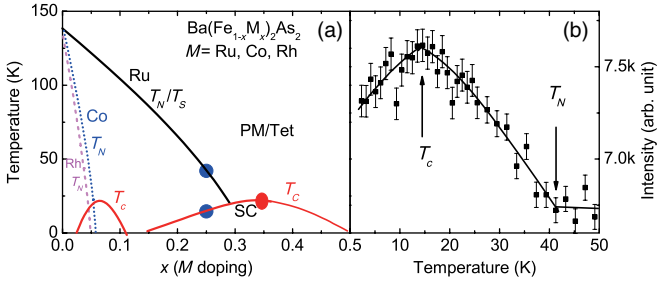

FIG. 1 (color online). (a) Schematic phase diagram of $Ba(Fe_{1-x}M_x)_2As_2$ $M =$ Ru, Co, Rh. The blue filled circles denote the T_c and T_N of the underdoped $Ba(Fe_{0.75}Ru_{0.25})_2As_2$ sample; the red filled circle denotes the T_c of optimally doped $Ba(Fe_{0.65}Ru_{0.35})_2As_2$ sample [3,16]. The blue dotted line and magenta dashed line denote the Néel temperatures of $Ba(Fe_{1-x}Co_x)_2As_2$ and $Ba(Fe_{1-x}Rh_x)_2As_2$, respectively [34]. (b) Temperature dependence of the intensity of magnetic Bragg peak (1/2, 1/2, 3) of the underdoped $Ba(Fe_{0.75}Ru_{0.25})_2As_2$ sample. The error bars indicate one standard deviation throughout the Letter.

doping [5]. Neutron scattering measurements also illustrate that the low energy magnetic excitations are dominated by a resonance mode [6–9]. In fact, the resonance mode is a universal feature for all high T_c superconductors and is believed to be important to Cooper pairing [5,10]. The resonance energy scales with T_c and the resonance spectral weight decreases with growth of the mismatch of the electron and hole Fermi surfaces [11,12]. These results are consistent with the scenario that the superconductivity is mediated by magnetic excitations between nested hole and electron Fermi surfaces and the resonance mode is directly associated with the Fermi surface nesting [5,11,12].

On the other hand, several ARPES measurements suggest that there are the same number of electrons and holes in $Ba(Fe_{1-x}Ru_x)_2As_2$, demonstrating that Ru doping indeed does not introduce extra holes or electrons [13,14]. The same measurements also find that the electron and hole Fermi surfaces are reasonably well nested over the whole phase diagram with Ru doping, in contrast to the carrier doped systems [13,14]. More interestingly, Hall and ARPES measurements have shown that the mobility of the carriers and the Fermi velocities in $Ba(Fe_{1-x}Ru_x)_2As_2$ increase dramatically as compared with those of $BaFe_2As_2$, indicating that the electron-electron interactions are further reduced under Ru doping [13]. All of these results suggest that isovalent doping tunes the properties of iron based superconductor in a different manner than that of carrier doping. However, little information is known about the evolution of the magnetic excitations and its relationship with the band structure and superconductivity under isovalent doping. Therefore, a study of the magnetic correlations in $Ba(Fe_{1-x}Ru_x)_2As_2$ is important to elucidate the physics of high T_c superconductivity in iron-based materials.

In this Letter, we report the doping dependence of the magnetic correlations in $Ba(Fe_{1-x}Ru_x)_2As_2$ ($x = 0.25$, $T_c = 14.5$ K; $x = 0.35$, $T_c = 20$ K) measured by elastic and inelastic neutron scattering techniques. We find that, while the magnitude and dispersion of the low energy spin gap in $Ba(Fe_{1-x}Ru_x)_2As_2$ are rather similar to those of the carrier doped counterparts, the resonance mode is significantly dampened. The overall magnetic excitation intensity in optimally doped $Ba(Fe_{0.65}Ru_{0.35})_2As_2$ is much weaker than that of electron doped counterparts [15]. Our result suggests that the reduction of the electron correlations by Ru substitution could be responsible for the suppression of the resonance mode, as well as the antiferromagnetic correlations.

$Ba(Fe_{1-x}Ru_x)_2As_2$ single crystals were grown out of self-flux with the nominal composition $x = 0.25$, 0.35. Magnetization measurements on several small pieces of each sample revealed superconducting transitions at $T_c = 14.5$ K and 20 K, respectively. Our neutron scattering measurements were performed on the HB-1 and HB-3 thermal triple axis spectrometers at the High Flux Isotope Reactor, and the BT-7 thermal triple axis spectrometer at the NIST Center for Neutron Research. We define the wave vector $\mathbf{Q}$ at (q_x, q_y, q_z) as $(h, k, l) = (q_x a/2\pi, q_y b/2\pi, q_z c/2\pi)$ reciprocal lattice units (r.l.u.) in the tetragonal unit cell. We used pyrolytic graphites (PGs) as monochromator and analyzer with the final neutron energy fixed at $E_f = 14.7$ meV.

The temperature dependence of the (1/2, 1/2, 3) magnetic Bragg peak in the $T_c = 14.5$ K sample shows that the upper limit of the Néel temperature is about 42 K [Fig. 1(b)], consistent with the phase diagram reported in the literature [Fig. 1(a)] [3,16]. Similar to carrier doped materials, the peak is partially suppressed below T_c, implying that the static antiferromagnetic order competes with superconductivity [12,17,18]. In the optimally doped $T_c = 20$ K sample, no static antiferromagnetic order is observed above 1.5 K.

For the inelastic measurements, we first turn to the $T_c = 14.5$ K sample. To investigate the momentum dependence of the spin excitations, we performed constant energy scans below and above T_c [Figs. 2(a) and 2(b)]. We find that the peak intensity is dramatically suppressed at $\hbar\omega = 2.5$ meV on cooling below T_c, while it increases only slightly at $\hbar\omega = 6$ meV. More surprisingly, the

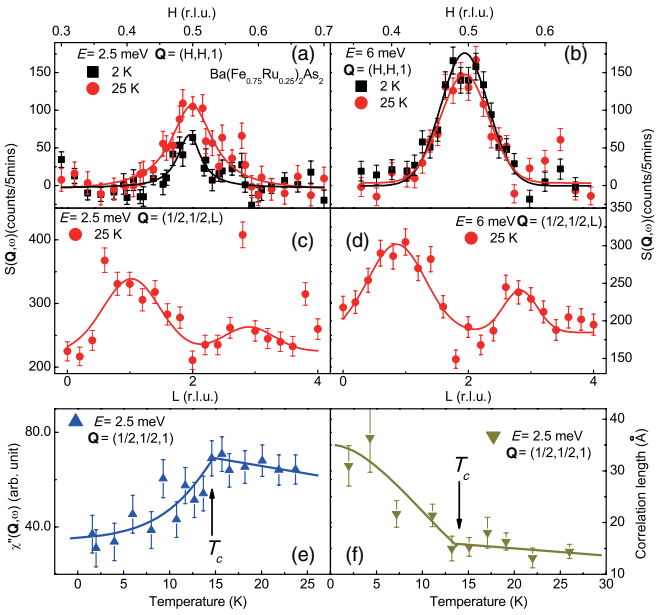

FIG. 2 (color online). Magnetic excitations in the $T_c = 14.5$ K sample. (a), (b) Constant energy scans near (1/2, 1/2, 1) below and above T_c; linear backgrounds are subtracted. (c), (d) L scans at 2.5 and 6 meV. (e) Temperature dependence of the dynamic susceptibility at (1/2, 1/2, 1) with $E = 2.5$ meV, which clearly shows a kink at T_c. The thermal population factor is corrected here. (f) Temperature dependence of the dynamical spin correlation length at 2.5 meV, which also displays a kink at T_c. The dynamical correlation length is estimated as 1/HWHM, where HWHM is the half width at half maximum of $\mathbf{Q}$scans deconvoluted with the instrumental resolution.

dynamical spin correlation length decreases significantly on warming above T_c at $\hbar\omega = 2.5$ meV while that of the $\hbar\omega = 6$ meV **Q**scan displays negligible changes across T_c. We carefully measured the temperature dependence of the dynamic susceptibility and the dynamical spin correlation length of the 2.5 meV **Q**scans [Figs. 2(e) and 2(f)]. These plots display superconducting order parameter-like temperature dependences and show kinks at T_c, suggesting that the opening of the spin gap and the increase of the dynamical correlation length are associated with the occurrence of superconductivity. These results also imply that the spin excitations are strongly coupled to the charge transport. It is possible to obtain a qualitative explanation of this phenomenon if we consider that the opening of the superconducting gap, which removes the interactions between electron and spin excitations below the gap, leads to the increase of the spin correlation length in the superconducting state. This is similar to the behavior of the phonons in conventional superconductors [19].

We also performed constant energy scans along L near the antiferromagnetic zone center [Figs. 2(c) and 2(d)]. We observe clear L modulations of the spin excitation intensities at both 2.5 meV and 6 meV. The K_z dependence of the band structure revealed by ARPES further confirmed the 3D nature of the system [13,14]. We notice that the dynamical spin correlation lengths in this sample are much shorter than that characterizing the spin wave excitations in the ordered parent compounds [20–23].

We now switch to the $T_c = 20$ K sample with no static antiferromagnetic order. The $\hbar\omega = 3$ meV **Q**scan near (1/2, 1/2, 1) displays a clear magnetic excitation peak in the normal state but is featureless in the superconducting state, suggesting the presence of a clean superconducting spin gap [Figs. 3(a) and 3(b)]. The magnetic signal at $\hbar\omega = 8$ meV increases slightly on cooling below T_c [Fig. 3(c)]. The temperature dependence of the scattering at $\hbar\omega = 8$ meV is clearly coupled with the occurrence of superconductivity [Fig. 3(d)].

Figure 4 summarizes the results for the dynamic susceptibility $\chi''(\mathbf{Q}, \omega)$ in absolute units normalized with acoustic phonons below and above T_c near the antiferromagnetic zone center (1/2, 1/2, L) in both samples. The low energy dynamic susceptibility $\chi''(\mathbf{Q}, \omega)$ in the normal state increases linearly with energy in the normal state in both samples [Figs. 4(a), 4(b), 4(e), and 4(f)], similar to the behavior in conventional weakly correlated antiferromagnetic metals [24]. To clarify the effect of superconductivity on the magnetic excitations, we subtract the normal state signal from the superconducting state signal. The outcome immediately reveals that spin gaps open below T_c. Above the spin gaps, resonant mode like weak enhancements are observed, although they are much less prominent as compared with those of the carrier doped superconductors [Figs. 4(c), 4(d), 4(g), and 4(h)] [9,15]. In the $T_c = 14.5$ K sample, the onset of the spin gap at $L = 0$ is

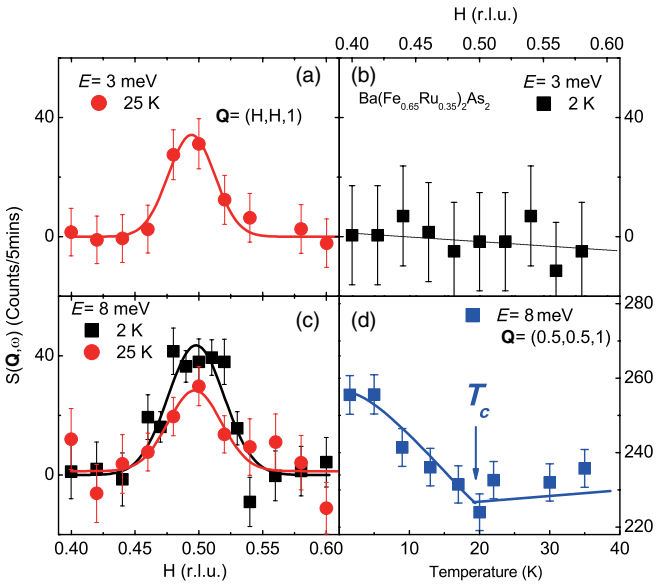

FIG. 3 (color online). Magnetic excitations in the $T_c = 20$ K sample. (a)–(c) Constant energy scans near (1/2, 1/2, 1) below and above T_c; linear backgrounds are subtracted. (d) Temperature dependence of magnetic excitation intensity at (1/2, 1/2, 1) with $\hbar\omega = 8$ meV, which clearly shows a kink at T_c.

4.5 meV, slightly larger than that (3.5 meV) at $L = 1$. The dispersion of the spin gap along the c axis may correlate to the variation of the superconducting gap along K_z in this underdoped sample, which is similar to the behavior of the carrier doped compounds [7,12]. The magnitudes of the spin gaps in the $T_c = 20$ K sample are slightly larger than those of the $T_c = 14.5$ K sample and the gap dispersion along the c axis persists in this sample. The total integrated spectral weights over the whole Brillouin zone up to 13 meV in the normal state for the underdoped and optimally doped $Ba(Fe_{1-x}Ru_x)_2As_2$ are about 0.0313 ± 0.009 and 0.0132 ± 0.004 μ_B^2/f.u., which are about 60% and 27% of that of the optimally doped $BaFe_{1.85}Co_{0.15}As_2$ at the same energy range, respectively [15]. More interestingly, although the magnitude of the spin gap in this system is comparable to those of the electron doped compounds with similar T_c, the resonance spectral weights [χ''(2 K)-χ''(25 K)] of the optimally doped and underdoped $Ba(Fe_{1-x}Ru_x)_2As_2$ are only about 0.00144 ± 0.0004 and 0.00175 ± 0.0005 μ_B^2/f.u., which are only 11% and 13% of that of $BaFe_{1.85}Co_{0.15}As_2$, respectively [15]. These results suggest that the Ru doping suppresses the magnetic correlations and resonance mode near the optimally doped regime significantly.

It is interesting to compare our results with those of the carrier doped high T_c superconductors and conventional BCS superconductors in the framework of the itinerant picture, where spin fluctuation arises mainly from the conduction electrons [10]. In the case of BCS superconductors, the singlet electron pairing is responsible for the reduction of the spin response below the superconducting

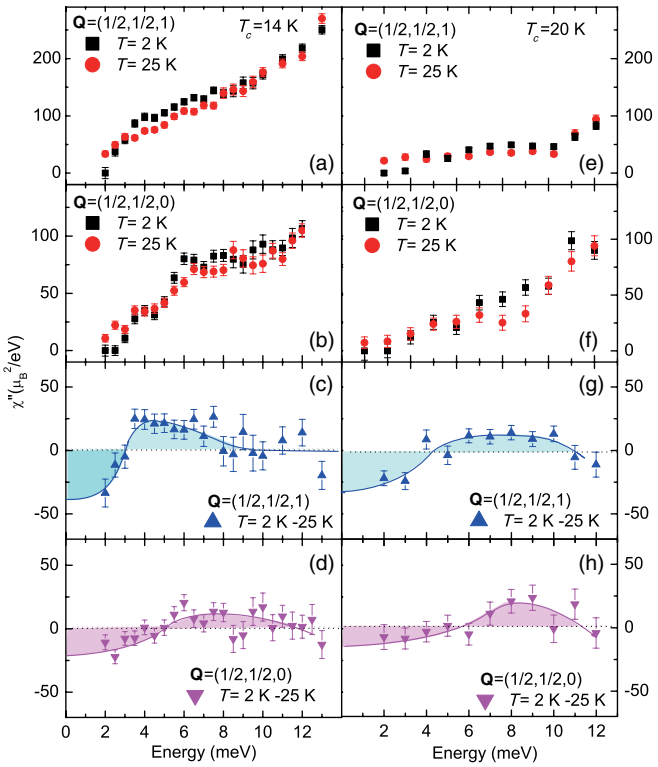

FIG. 4 (color online). (a), (b) Imaginary part of the dynamic susceptibility $\chi''(\mathbf{Q}, \omega)$ in the superconducting state (2 K) and normal state (25 K) of the $T_c = 14.5$ K sample. The data were obtained by correcting the thermal population factor. (c), (d) Temperature difference plots of the dynamic susceptibility between 2 K and 25 K at $\mathbf{Q} = (1/2, 1/2, 1)$ and $\mathbf{Q} = (1/2, 1/2, 0)$ of the $T_c = 14.5$ K sample. (e), (f) Imaginary part of the dynamic susceptibility $\chi''(\mathbf{Q}, \omega)$ in the superconducting state and normal state of the $T_c = 20$ K sample. (g), (h) Temperature difference plots of the dynamic susceptibility between 2 K and 25 K at $\mathbf{Q} = (1/2, 1/2, 1)$ and $\mathbf{Q} = (1/2, 1/2, 0)$ of the $T_c = 20$ K sample. The shaded area denotes the spectral weight change below and above T_c. In both samples, the energy dependent background measured near $\mathbf{Q} = (0.7, 0.7, L)$ are subtracted and all magnetic intensities are normalized to absolute units with acoustic phonons.

gap (2Δ) in the superconducting state. When the Cooper pair binding energy (2Δ) is exceeded, the spin response is enhanced. The enhanced spin excitations are usually very broad in momentum and energy because of the large bandwidth and weak correlations in conventional superconductors. In the carrier-doped iron-based superconductors, a sharp spin resonance with an energy $\hbar\omega_r$ appears below the superconducting gap ($\hbar\omega_r < 2\Delta$) caused by coherence factors introduced by pairing [25,26] and a spin gap (Δ_s) opens below the resonance mode energy ($\Delta_s < \hbar\omega_r \leq 2\Delta$) [6–9]. At first glance, a weak resonance is not expected in $Ba(Fe_{1-x}Ru_x)_2As_2$, since the Fermi surfaces are nested reasonably well [11–14]. However, in the random phase approximation (RPA), the resonance mode spectral weight and energy are also affected by the effective electron-electron interactions U_{eff} [10]. The resonance spectral weight diminishes with decreasing U_{eff}. Because the Ru doping is expected to reduce the electron-electron interactions due to the large spatial extension of the Ru $4d$ orbitals and stronger d-p hybridization of the Ru and As, as confirmed by ARPES and Hall measurements [13,14], it is very likely that the weakening of the electron correlations results in the dampening of the resonance mode near the optimally doped regime. Additionally, the resonance mode ($\hbar\omega_r$) will shift toward 2Δ as U_{eff} decreases, which leads to the increase in the magnitude of the spin gap. As a result, although the resonance mode is broadened in energy and dampened in intensity, a relatively large spin gap can persist in $Ba(Fe_{1-x}Ru_x)_2As_2$. These also explain why the resonance intensity is much stronger in strongly correlated hole doped cuprates (such as YBCO and Bi2212) than those of the moderately correlated electron doped cuprates (PLCCO and NCCO) and carrier doped iron-based superconductors [15,27–33].

By taking the electron correlation effect into account, we may qualitatively understand the magnetic phase diagram in $Ba(Fe_{1-x}Ru_x)_2As_2$ and other carrier doped compounds. The weakening of the electron correlations by Ru doping is expected to reduce the density of states near the Fermi surfaces and the Stoner enhancement, which leads to the suppression of the antiferromagnetic correlations. In the case of carrier doped compounds, the carrier doping not only weakens the Fermi surface nesting but also reduces the electron correlations, and both effects suppress the antiferromagnetic correlations. This naturally accounts for the fact that the magnetic phase diagram in $Ba(Fe_{1-x}Ru_x)_2As_2$ is much broader than those of the electron-doped iron-based superconductors [Fig. 1(a)]. We also notice that, due to the extended $4d$ orbitals of Rh, the suppression of the antiferromagentic order by Rh substitution is more dramatic than that by Co substitution, although both Rh and Co have similar electron configurations (each has one extra electron than Fe) [Fig. 1(a)] [34]. Therefore, it becomes evident that both Fermi surface nesting and electron correlations play important roles in controlling the magnetic phase diagram of iron-based superconductors.

On the other hand, it has also been speculated that the Ru doping may act like a magnetic dilution or impurity, which can also suppress antiferromagnetic order without detuning the nesting condition [35]. However, this is inconsistent with the fact that the Fermi velocities and the carrier mobility increase under Ru doping [13,14]. And, in this approach, it seems difficult to explain the presence of the large superconducting spin gap observed here. Apparently, doping impurities would be expected to induce density of states at low energies and close the spin gap, just like those discovered in cuprates and iron chalcogenides [36–38]. Very recently, thermal conductivity measurements have suggested that similar nodal superconductivity occurs in

isovalently doped $Ba(Fe_{1-x}Ru_x)_2As_2$ and $BaFe_2(As_{1-x}P_x)_2$ (Ref. [39]). ARPES measurements also showed that a horizontal line node is located at the Z point $(0, 0, \pi)$ in the hole band in $BaFe_2(As_{1-x}P_x)_2$ (Ref. [40]). This horizontal line node only affects a small area of the Fermi surface and has little impact on the magnetic correlations and resonance mode. The presence of a relatively large superconducting spin gap in optimally doped $Ba(Fe_{0.65}Ru_{0.35})_2As_2$ also indicates that the majority of the Fermi surface is still fully gapped. Hence, the reduction of the electron correlations seems to be a more important reason leading to the suppression of antiferromagetic correlations and the resonance mode in $Ba(Fe_{1-x}Ru_x)_2As_2$. In any case, the coexistence of the superconductivity, superconducting spin gap and dampened resonance mode implies that the resonance is the consequence of the strong electron correlations of high T_c superconductors, rather than the only ingredient involved in the electron pairing.

In summary, we have characterized the low energy spin excitations in isovalently doped $Ba(Fe_{1-x}Ru_x)_2As_2$ below and above T_c. We find that the Ru doping, which weakens the electron correlations, leads to dramatic suppression of the resonance mode and normal state antiferromagnetic correlations near the optimally doped regime in the system.

We thank D. H. Lee, H. Yao, and Y. M. Xu for useful discussions. This work is supported by the Director, Office of Science, Office of Basic Energy Sciences, U.S. Department of Energy, under Contract No. DE-AC02-05CH11231 and Office of Basic Energy Sciences US DOE DE-AC03-76SF008. Jun Zhao is supported by Miller Institute for Basic Research in Science and Thousand Young Talents Program. The research at ORNL's HFIR was sponsored by the Scientific User Facilities Division, Office of Basic Energy Sciences, U.S. Department of Energy.

[1] M. A. Kastner, R. Birgeneau, G. Shirane, and Y. Endoh, Rev. Mod. Phys. **70**, 897 (1998).
[2] D. Johnston, Adv. Phys. **59**, 803 (2010).
[3] M. G. Kim *et al.*, Phys. Rev. B **83**, 054514 (2011).
[4] A. Thaler, N. Ni, A. Kracher, J. Q. Yan, S. L. Bud'ko, and P. C. Canfield, Phys. Rev. B **82**, 014534 (2010).
[5] K. Terashima *et al.*, Proc. Natl. Acad. Sci. U.S.A. **106**, 7330 (2009).
[6] A. Christianson *et al.*, Nature (London) **456**, 930 (2008).
[7] S. Chi *et al.*, Phys. Rev. Lett. **102**, 107006 (2009).
[8] M. D. Lumsden *et al.*, Phys. Rev. Lett. **102**, 107005 (2009).
[9] J. Zhao, L.-P. Regnault, C. Zhang, M. Wang, Z. Li, F. Zhou, Z. Zhao, C. Fang, J. Hu, and P. Dai, Phys. Rev. B **81**, 180505(R) (2010).
[10] M. Eschrig, Adv. Phys. **55**, 47 (2006).
[11] J.-P. Castellan *et al.*, Phys. Rev. Lett. **107**, 177003 (2011).
[12] M. Wang *et al.*, Phys. Rev. B **81**, 174524 (2010).
[13] V. Brouet *et al.*, Phys. Rev. Lett. **105**, 087001 (2010).
[14] N. Xu *et al.*, Phys. Rev. B **86**, 064505 (2012).
[15] D. S. Inosov *et al.*, Nat. Phys. **6**, 178 (2009).
[16] F. Rullier-Albenque, D. Colson, A. Forget, P. Thuéry, and S. Poissonnet, Phys. Rev. B **81**, 224503 (2010).
[17] D. K. Pratt, W. Tian, A. Kreyssig, J. Zarestky, S. Nandi, N. Ni, S. Bud'ko, P. Canfield, A. Goldman, and R. McQueeney, Phys. Rev. Lett. **103**, 087001 (2009).
[18] A. Christianson, M. Lumsden, S. Nagler, G. MacDougall, M. McGuire, A. Sefat, R. Jin, B. Sales, and D. Mandrus, Phys. Rev. Lett. **103**, 087002 (2009).
[19] F. Weber and L. Pintschovius, Phys. Rev. B **82**, 024509 (2010).
[20] J. Zhao *et al.*, Phys. Rev. Lett. **101**, 167203 (2008).
[21] J. Zhao, D. T. Adroja, D.-X. Yao, R. Bewley, S. Li, X. F. Wang, G. Wu, X. H. Chen, J. Hu, and P. Dai, Nat. Phys. **5**, 555 (2009).
[22] K. Matan, R. Morinaga, K. Iida, and T. J. Sato, Phys. Rev. B **79**, 054526 (2009).
[23] L. W. Harriger, H. Q. Luo, M. S. Liu, C. Frost, J. P. Hu, M. R. Norman, and P. Dai, Phys. Rev. B **84**, 054544 (2011).
[24] T. Moriya, *Spin Fluctuations in Itinerant Electron Magnetism* (Springer-Verlag, Berlin/Heidelberg, 1985).
[25] M. M. Korshunov and I. Eremin, Phys. Rev. B **78**, 140509 (2008).
[26] T. A. Maier, S. Graser, D. Scalapino, and P. Hirschfeld, Phys. Rev. B **79**, 134520 (2009).
[27] J. Zhao *et al.*, Nat. Phys. **7**, 719 (2011).
[28] R. J. Birgeneau, C. Stock, J. M. Tranquada, and K. Yamada, J. Phys. Soc. Jpn. **75**, 111003 (2006).
[29] H. F. Fong, P. Bourges, Y. Sidis, L. Regnault, J. Bossy, A. Ivanov, D. Milius, I. Aksay, and B. Keimer, Phys. Rev. B **61**, 14 773 (2000).
[30] P. C. Dai, H. Mook, R. Hunt, and F. Doğan, Phys. Rev. B **63**, 054525 (2001).
[31] S. D. Wilson, P. Dai, S. Li, S. Chi, H. J. Kang, and J. W. Lynn, Nature (London) **442**, 59 (2006).
[32] J. Zhao, P. Dai, S. Li, P. G. Freeman, Y. Onose, and Y. Tokura, Phys. Rev. Lett. **99**, 017001 (2007).
[33] H. F. Fong, H. F. Fong, P. Bourges, Y. Sidis, L. P. Regnault, A. Ivanov, G. D. Gu, and N. Koshizuka, Nature (London) **398**, 588 (1999).
[34] N. Ni, A. Thaler, A. Kracher, J. Yan, S. Bud'ko, and P. Canfield, Phys. Rev. B **80**, 024511 (2009).
[35] R. S. Dhaka *et al.*, Phys. Rev. Lett. **107**, 267002 (2011).
[36] A. Suchaneck *et al.*, Phys. Rev. Lett. **105**, 037207 (2010).
[37] H. Kimura, M. Kofu, Y. Matsumoto, and K. Hirota, Phys. Rev. Lett. **91**, 067002 (2003).
[38] Z. Xu *et al.*, Phys. Rev. Lett. **109**, 227002 (2012).
[39] X. Qiu *et al.*, Phys. Rev. X **2**, 011010 (2012).
[40] Y. Zhang, Z. R. Ye, Q. Q. Ge, F. Chen, J. Jiang, M. Xu, B. P. Xie, and D. L. Feng, Nat. Phys. **8**, 371 (2012).